Role of VEGF in maintaining renal structure and function under normotensive and hypertensive conditions

Andrew Advani*†‡, Darren J. Kelly†, Suzanne L. Advani*†‡, Alison J. Cox†, Kerri Thai*, Yuan Zhang†, Kathryn E. White‡, Renae M. Gow†, Sally M. Marshall‡, Brent M. Steer*, Philip A. Marsden*, P. Elizabeth Rakoczy§, and Richard E. Gilbert*†¶

*Department of Medicine, University of Toronto, St. Michael's Hospital, Toronto, ON, Canada M5C 2T2; †Department of Medicine, University of Melbourne, St. Vincent's Hospital, Victoria 3065, Australia; ‡School of Clinical Medical Sciences, Medical School, Newcastle University, Newcastle upon Tyne NE2 4HH, United Kingdom; and §Centre for Ophthalmology and Visual Science, University of Western Australia, Nedlands, WA 6009, Australia

Edited by Solomon H. Snyder, Johns Hopkins University School of Medicine, Baltimore, MD, and approved July 15, 2007 (received for review April 20, 2007)

Inhibiting the actions of VEGF is a new therapeutic paradigm in cancer management with antiangiogenic therapy also under intensive investigation in a range of nonmalignant diseases characterized by pathological angiogenesis. However, the effects of VEGF inhibition on organs that constitutively express it in adulthood, such as the kidney, are mostly unknown. Accordingly, we examined the effect of VEGF inhibition on renal structure and function under physiological conditions and in the setting of the common renal stressors: hypertension and activation of the renin–angiotensin system. When compared with normotensive Sprague–Dawley (SD) rats, glomerular VEGF mRNA was increased 2-fold in transgenic (mRen-2)27 rats that overexpress renin with spontaneously hypertensive rat (SHR) kidneys showing VEGF expression levels that were intermediate between them. Administration of either an orally active inhibitor of the type 2 VEGF receptor (VEGFR-2) tyrosine kinase or a VEGF neutralizing antibody to TGR(mRen-2)27 rats resulted in loss of glomerular endothelial cells and transformation to a malignant hypertensive phenotype with severe glomerulosclerosis. VEGFR-2 kinase inhibition treatment was well tolerated in SDs and SHRs; although even in these animals there was detectable endothelial cell loss and rise in albuminuria. Mild mesangial expansion was also noted in hypertensive SHR, but not in SD rats. These studies illustrate: (*i*) VEGF has a role in the maintenance of glomerular endothelial integrity under physiological circumstances, (*ii*) glomerular VEGF is increased in response to hypertension and activation of the renin–angiotensin system, and (*iii*) VEGF signaling plays a protective role in the setting of these renal stressors.

albuminuria | endothelium | hypertension | Ren-2 | renin–angiotensin system

VEGF is a proangiogenic growth factor essential for embryonic development (1, 2). Traditionally, constitutively expressed VEGF has been thought to have a limited role in normal adult physiology (3), although recent studies have begun to challenge this view (4, 5).

Angiogenic growth factors like VEGF are pivotal in the neoangiogenesis that is central to the progression of many malignancies. Indeed, based on encouraging results from a number of cancer trials (6), VEGF inhibition is currently in widespread use in oncology practice. Moreover, anti-VEGF therapy is also under investigation for a range of nonmalignant diseases characterized by disordered angiogenesis, such as rheumatoid arthritis, proliferative diabetic retinopathy, and age-related macular degeneration (7).

Gene deletion and antibody-based studies have provided compelling evidence for VEGF's pivotal role in the developmental regulation of the glomerular capillary network (8, 9). However, the actions of VEGF in the normal adult kidney are less well established, and its role in renal disease is controversial. For instance, as a consequence of its ability to induce vascular permeability (10), monocyte chemotaxis (11), and vasodilatation (12), VEGF has been implicated in the pathogenesis of kidney disease. In contrast, other studies have suggested a renoprotective effect of VEGF in albeit relatively rare conditions such as thrombotic microangiopathy (13) and crescentic glomerulonephritis (14). Essential hypertension, by way of contrast, is a common renal stressor in which the function of constitutively expressed VEGF has not previously been investigated. Moreover, an extensive body of experimental and clinical studies has also highlighted the renin–angiotensin system (RAS) as a common and important renal stressor, beyond its apparent effects on blood pressure (15). Accordingly, we first examined the expression of VEGF and its receptor in a rodent model of essential hypertension and another model with increased activity of the RAS, the transgenic (mRen-2)27 rat (16). We then determined the effects of VEGF inhibition on kidney function and structure. The results suggest a role for constitutive VEGF in protecting the kidney from the injurious effects of hypertension and the RAS that might have important implications for the future development of VEGF inhibitory strategies.

Results

Renal Expression of VEGF and VEGF Receptor (VEGFR)-2. Glomerular VEGF gene expression was 2-fold higher in TGR(mRen-2)27 compared with Sprague–Dawley (SD) rats, with spontaneously hypertensive rat (SHR) kidneys showing VEGF mRNA levels that were intermediate between them [Fig. 1 (Glomerular VEGF-A expression, normalized to control (SD), $n = 10$–17 per group: SD 1.00 ± 0.13, SHR 1.62 ± 0.21, TGR(mRen-2)27 2.11 ± 0.23 ($P < 0.01$ vs. SD)]. In contrast, there was no difference in glomerular VEGFR-2 expression between groups [see supporting information (SI) Fig. 8]. Light microscopy after *in situ* hybridization confirmed abundant VEGF expression within the podocytes with VEGFR-2 mRNA found principally in glomerular endothelial cells.

Expression of glomerular VEGF was significantly lower in kidney sections from TGR(mRen-2)27 rats that had been treated with the

Author contributions: A.A. and D.J.K. contributed equally to this work; A.A., D.J.K., and R.E.G. designed research; A.A., S.L.A., A.J.C., K.T., Y.Z., K.E.W., and R.M.G. performed research; D.J.K., S.M.M., B.M.S., P.A.M., P.E.R., and R.E.G. contributed new reagents/analytic tools; A.A., D.J.K., A.J.C., K.E.W., and R.E.G. analyzed data; and A.A. and R.E.G. wrote the paper.

Conflict of interest statement: A.A. and R.E.G. have received travel grants to attend scientific meetings from AstraZeneca, the manufacturer of vandetanib, one of the compounds used in this study.

This article is a PNAS Direct Submission.

Abbreviations: VEGFR, VEGF receptor; SHR, spontaneously hypertensive rats; SD, Sprague–Dawley; SBP, systolic blood pressure; GFR, glomerular filtration rate; AER, albumin excretion rate; GSI glomerulosclerosis index; LCM, laser capture microdissection.

¶To whom correspondence should be addressed at: Department of Medicine, University of Toronto, Division of Endocrinology, St. Michael's Hospital, 61 Queen Street East, Toronto, ON, Canada M5C 2T2. E-mail: richard.gilbert@utoronto.ca.

This article contains supporting information online at www.pnas.org/cgi/content/full/0703577104/DC1.

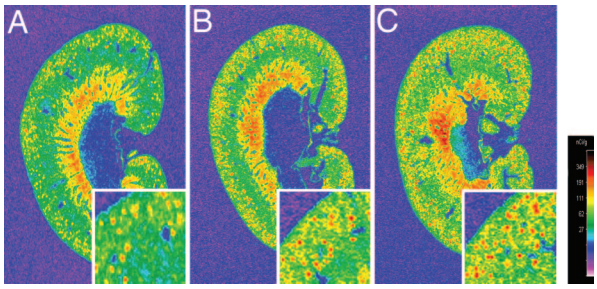

Fig. 1. *In situ* hybridization autoradiographs of kidney sections probed for VEGF-A. (*A*) SD rat. (*B*) SHR. (*C*) TGR(mRen-2)27 rat.

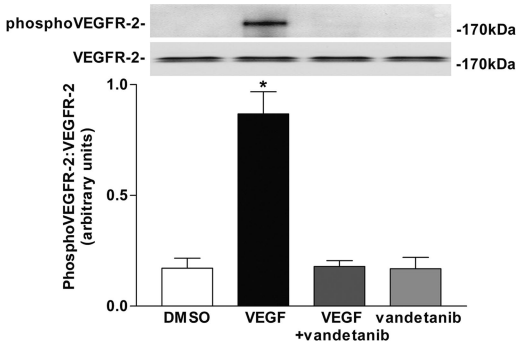

Fig. 2. Effect of VEGF and vandetanib on VEGFR-2 phosphorylation in cultured human glomerular endothelial cells. *, $P < 0.001$ vs. all other groups (mean of three experiments).

ACE inhibitor perindopril, compared with age-matched controls (*SI Methods* and SI Fig. 9).

Effect of Vandetanib on VEGFR-2 Phosphorylation *in Vitro*. VEGF administration resulted in a significant increase in VEGFR-2 phosphorylation in cultured human glomerular endothelial cells. This increase was abolished by preincubation of cells with the VEGFR-2 kinase inhibitor vandetanib (ZACTIMA; ZD6474) (Fig. 2).

Renal Function. Systolic blood pressure (SBP) was higher in SHR and TGR(mRen-2)27 than SD rats (Table 1). Treatment of either SD rats or SHR with vandetanib was well tolerated, whereas in TGR(mRen-2)27 rats, it resulted in marked reduction in glomerular filtration rate (GFR), increased plasma creatinine, heavy proteinuria, and increased mortality (in excess of 50%) not seen in SHR or SD animals (Table 1). Although total urinary protein was not increased, vandetanib nevertheless led to an increase in urinary albumin excretion rate in both SHR and SD rats when compared with their vehicle-treated counterparts (Table 1).

Endothelial Cell Density. Examination of kidney sections stained with the endothelial cell marker JG-12 showed intense staining of glomerular capillaries with no difference between the three vehicle-treated groups (Fig. 3). Vandetanib administration was associated with an overall reduction in glomerular endothelial staining in all three groups. However, whereas there was a small but significant reduction in glomerular endothelial cell staining in SD rats, it was more pronounced in SHR and greatest in TGR(mRen-2)27 rats (Fig. 3).

Glomerular Endothelial Cell Ultrastructure. In TGR(mRen-2)27 rats, vandetanib administration resulted in near-complete loss of glomerular endothelial cells as assessed by transmission electron microscopy (Fig. 4). Endothelial apoptotic changes were also evident in SHR after vandetanib treatment, although injury was not as prominent as in TGR(mRen-2)27 rats. Ultrastructural changes in glomerular endothelial cells from vandetanib-treated SD rats were limited to some loss of characteristic fenestrae (Fig. 4 *G* and *H*) as reported for VEGF receptor tyrosine kinase inhibition (4).

Histopathology. Vehicle-treated TGR(mRen-2)27 rats showed only mild basement membrane thickening and mesangial expansion. In contrast, kidneys taken from TGR(mRen-2)27 rats treated with vandetanib revealed changes reminiscent of malignant hypertension with fibrinoid necrosis of afferent arterioles, concentric myointimal proliferation, and collagen deposition (Fig. 5). There was marked glomerular and cortical interstitial macrophage infiltration with fibrin deposition (Fig. 5) and severe glomerulosclerosis (SI Fig. 10). By contrast, vandetanib-treated SHR showed only a mild degree of mesangial expansion. No significant changes in glomerular morphology were noted in SD rats (SI Fig. 10).

In addition to the kidney, proliferative myointimal changes were also observed within the heart, lungs, mesentery, and testes of TGR(mRen-2)27 rats treated with vandetanib. However, pathological changes within the brain, liver, spleen, aorta, or duodenum were infrequent. Microangiopathic hemolytic anemia (red cell fragmentation, polychromasia, and nucleated red cells) was also seen in some TGR(mRen-2)27 rats receiving vandetanib.

Administration of vandetanib at a lower dose (15 mg/kg/day) to TGR(mRen-2)27 rats also resulted in histopathological changes of malignant hypertension (mortality 6 of 18) with decline in GFR, heavy proteinuria, and loss of endothelial cells, even though SBP was not different to that observed in vehicle-treated TGR(mRen-2)27 rats (*SI Methods* and SI Fig. 11).

Effects of Vandetanib on Glomerular Podocytes. Podocyte density was lower in SHR and TGR(mRen-2)27 rats than SD rats (Table 2 and SI Fig. 12). Although vandetanib administration did not cause a reduction in total podocyte density in SD, SHR, or TGR(mRen-2)27 rats, structural evidence of podocyte injury was present in all three groups. Defects in podocyte morphology in SD rats were restricted to the presence of occasional pseudocysts, whereas in SHR, there were proteinaceous adsorption droplets (Fig. 6 and

Table 1. Renal function parameters, SBP, and survival of SD, SHR, and TGR(mRen-2)27 rats at the end of the study period

Animal/treatment	Alive/dead	SBP, mmHg	Plasma creatinine, mmol/liter	GFR, ml/min/kg	AER, mg/day	Proteinuria, mg/day
SD + vehicle	12/0	118 ± 3	0.030 ± 0.002	11.40 ± 0.24	0.29 ×/÷ 1.21	13.4 ×/÷ 1.1
SD + vandetanib	12/0	127 ± 5	0.038 ± 0.001	10.12 ± 0.39	1.02 ×/÷ 1.30*	15.7 ×/÷ 1.4
SHR + vehicle	14/0	185 ± 5†	0.037 ± 0.002	9.75 ± 0.21	0.46 ×/÷ 1.21	23.8 ×/÷ 1.1
SHR + vandetanib	14/0	200 ± 7	0.041 ± 0.001	9.92 ± 0.23	4.19 ×/÷ 1.19‡	28.1 ×/÷ 1.1
TGR(mRen-2)27 + vehicle	19/0	202 ± 5†§	0.041 ± 0.004¶	10.46 ± 0.63	21.68 ×/÷ 1.45†‡	38.8 ×/÷ 1.2†‖
TGR(mRen-2)27 + vandetanib	16/20**	223 ± 7	0.058 ± 0.002††	5.98 ± 0.53††	158.86 ×/÷ 1.14††	133.7 ×/÷ 1.2††

Albumin excretion rate (AER) and proteinuria expressed as geometric mean × /÷ tolerance factors. *, $P < 0.01$ vs. SD + vehicle; †, $P < 0.001$ vs. SD + vehicle; ‡, $P < 0.001$ vs. SHR + vehicle; §, $P < 0.05$ vs. SHR + vehicle; ¶, $P < 0.05$ vs. SD + vehicle; ‖, $P < 0.01$ vs. SHR + vehicle; **, $P < 0.01$ vs. TGR(mRen-2)27 + vehicle; ††, $P < 0.001$ vs. TGR(mRen-2)27 + vehicle.

MEDICAL SCIENCES

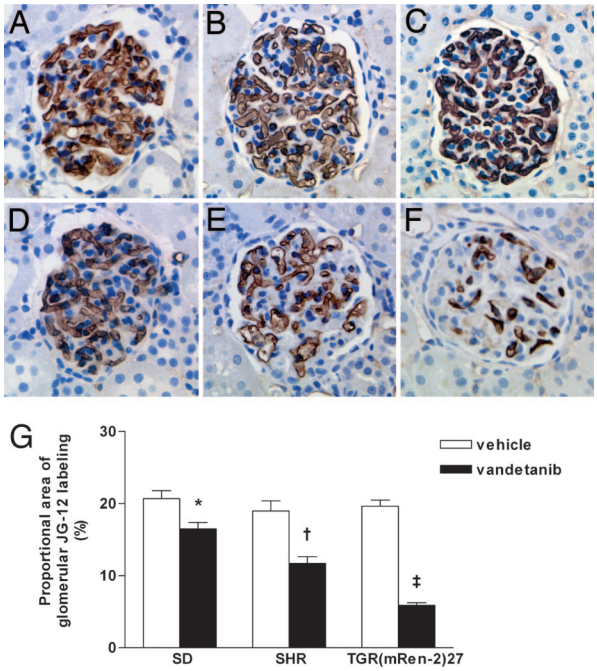

Fig. 3. Endothelial cell immunohistochemistry (JG-12 labeling) in kidney sections from vehicle-treated animals. (*A–C*) SD rat (*A*), SHR (*B*), TGR(mRen-2)27 rat (*C*). (*D–F*) After vandetanib, SD rat (*D*), SHR (*E*), and TGR(mRen-2)27 rat (*F*). (Magnification: ×400.) (*G*) Quantitative assessment of glomerular capillary endothelial density, $n = 10$ per group. *, $P < 0.05$ vs. SD + vehicle; †, $P < 0.001$ vs. SHR + vehicle; ‡, $P < 0.001$ vs. TGR(mRen-2)27 + vehicle.

Table 2). Severe glomerulosclerosis in TGR(mRen-2)27 rats was associated with abundant pseudocyst formation and adsorption droplets in podocytes with some foot process fusion.

Glomerular Gene Expression. To investigate the mechanisms underlying the development of albuminuria in vandetanib-treated rats, we examined the gene expression of the slit-pore associated protein nephrin; perlecan, a protein that contributes to the charge selectivity of the filtration barrier; and Ret kinase, a prosurvival factor for podocytes that is also inhibited by vandetanib. Although nephrin mRNA was increased in hypertensive rats (SHR and TGR(mRen-2)27) its abundance was unchanged by vandetanib (Table 2 and SI Fig. 13). There was no difference between vehicle-treated animal groups in the renal expression of perlecan (fold change relative to SD: SD 1.1 ± 0.3, SHR 1.0 ± 0.1, TGR(mRen-2)27 0.8 ± 0.1). Although perlecan expression was still present in glomeruli after vandetanib treatment in SD and SHR animals, it was undetectable in TGR(mRen-2)27 rats with vandetanib after 40 PCR cycles (Fig. 7). We were unable to detect the presence of Ret in glomeruli from SD, SHR, or TGR(mRen-2)27 rats.

Effect of VEGF Neutralizing Antibody in TGR(mRen-2)27 Rats. Treatment of TGR(mRen-2)27 rats with a VEGF neutralizing antibody also resulted in development of malignant hypertension with worsening proteinuria not observed in animals treated with normal IgG (SI Fig. 14 *A–D*). In comparison with controls, VEGF neutralizing antibody-treated TGR(mRen-2)27 rats had a greater rise in SBP and decline in GFR. As observed with vandetanib, there was endothelial cell dropout on JG12 labeling with significant mesangial expansion, myointimal proliferation of the afferent arterioles, and fibrinoid necrosis (SI Fig. 14 *E–L*). Ultrastructurally, there was evidence of endothelial cell apoptosis with remnant nuclei and cytoplasmic vacuolization as well as pseudocyst and adsorption droplet accumulation within podocytes (SI Fig. 14*M*).

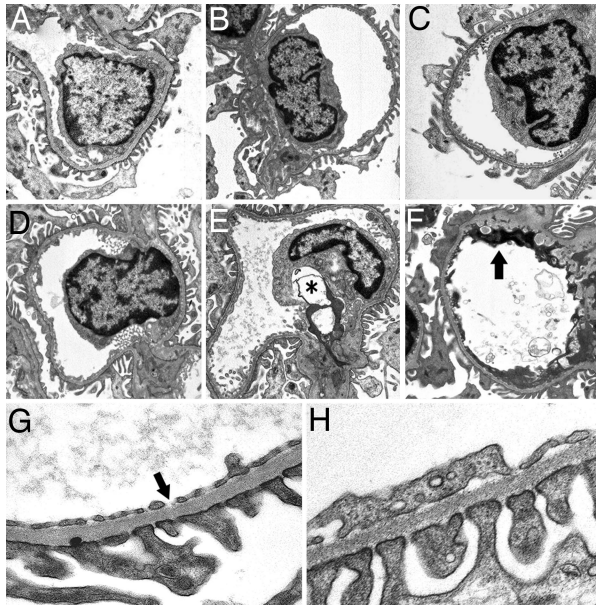

Fig. 4. Transmission electron micrographs of representative glomerular endothelial cells from vehicle-treated animals. (*A–C*) SD rat (*A*), SHR (*B*), TGR(mRen-2)27 rat (*C*). (*D–F*) After vandetanib, SD rat (*D*), SHR (*E*), and TGR(mRen-2)27 rat (*F*). Among vandetanib-treated groups, some changes in glomerular endothelial cell morphology could be seen in SHR (cytoplasmic vacuoles, asterisk), whereas in TGR(mRen-2)27 rats there was marked injury with remnant nuclei indicative of apoptosis (arrow). (Magnification: ×8,900.) (*G* and *H*) Transmission electron micrographs from SD rats treated with vehicle (*G*) and vandetanib (*H*). Vehicle-treated animals showed characteristic endothelial cell fenestrae (arrow). In contrast, fewer fenestrae were apparent after vandetanib. (Magnification: ×28,500.)

Discussion

In addition to advancing our knowledge of cardiovascular pathophysiology, understanding the role of VEGF has special relevance in light of the numerous new therapies that aim to enhance or diminish its action. Our findings suggest that VEGF up-regulation in response to hypertension, and especially hypertension mediated through activation of the RAS, may be beneficial and that VEGF blockade may accelerate the progression of kidney disease.

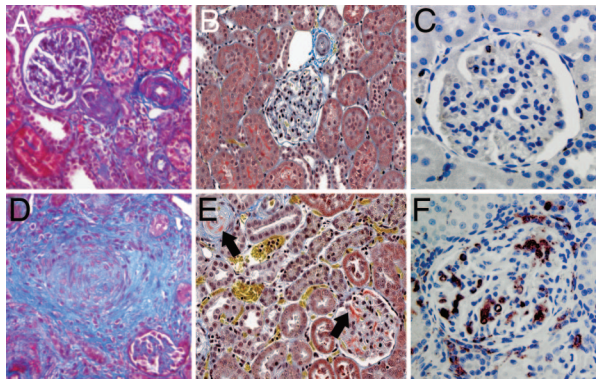

Fig. 5. Kidney sections from TGR(mRen-2)27 rats treated with vehicle (*A–C*) and after vandetanib (*D–F*), stained with Masson's trichrome (*A* and *D*; magnification ×200), Martius scarlet blue (*B* and *E*; magnification ×200) and after ED-1 labeling (*C* and *F*; magnification ×400). Vandetanib treatment led to myointimal proliferation and collagen deposition (blue, *D*), with intraarteriolar and intraglomerular fibrin deposition (red, arrow, *E*). ED1 immunostaining showed glomerular and cortical interstitial macrophage infiltration with vandetanib (*F*).

Table 2. Podocyte characteristics in SD, SHR, and TGR(mRen-2)27 rats after treatment with vehicle or vandetanib

Animal/treatment	Podocyte density, N_v ($\times 10^{-5}$ per μm^{-3})	WT1-positive nuclei per glomerular profile	Abnormal podocytes per field	Glomerular nephrin expression
SD + vehicle	23 ± 2	8.8 ± 0.4	0.08 ± 0.04	1.00 ± 0.07
SD + vandetanib	26 ± 4	9.2 ± 0.3	0.44 ± 0.17	1.33 ± 0.22
SHR + vehicle	14 ± 2	5.1 ± 0.4*	0.18 ± 0.07	1.94 ± 0.18†
SHR + vandetanib	18 ± 4	5.9 ± 0.3	1.51 ± 0.52‡	2.32 ± 0.55
TGR(mRen-2)27 + vehicle	11 ± 2§	5.4 ± 0.2*	0.25 ± 0.03	1.69 ± 0.25§
TGR(mRen-2)27 + vandetanib	13 ± 7	5.5 ± 0.6	2.79 ± 0.29¶	2.39 ± 0.55

Podocyte density (N_v, numerical density) determined by electron microscopy using the Weibel–Gomez method. Glomerular nephrin normalized to SD + vehicle (n = 9–12 per group). *, $P < 0.001$ vs. SD + vehicle; †, $P < 0.01$ vs. SD + vehicle; ‡, $P < 0.05$ vs. SHR + vehicle; §, $P < 0.05$ vs. SD + vehicle; ¶, $P < 0.001$ vs. TGR(mRen-2)27 + vehicle.

To examine the contributions of hypertension and angiotensin II to VEGF expression, we used two genetic models of hypertension. Both plasma and intrarenal angiotensin II are increased in TGR(mRen-2)27 rats (16). In contrast, the SHR is viewed as a model of sympathoadrenal-mediated hypertension in which both circulating and kidney angiotensin II are reduced (17). We found that, in comparison with controls, glomerular VEGF mRNA was increased in SHRs, and to an even greater extent in TGR(mRen-2)27 rats, but reduced with ACE inhibition. *In vivo* and *in vitro* studies have shown that both mechanical stretch and angiotensin II potently stimulate the expression of VEGF (18, 19). Accordingly, VEGF upregulation may represent an adaptive response to hypertension, possibly through effects on vascular relaxation. VEGF causes an increase in endothelial nitric oxide (NO) synthase expression (20), and inhibiting NO accelerates renal disease. Furthermore, NO inhibition causes an increase in VEGF synthesis in vascular smooth muscle cells under hypoxic conditions, suggesting that this may be an important intermediary (21).

When the actions of VEGF were blocked, SHRs and TGR(mRen-2)27 rats, respectively, developed mild and severe glomerulosclerosis, signifying that VEGF may be important in maintaining glomerular integrity in the hypertensive setting. Unlike the relatively benign changes in SHRs, TGR(mRen-2)27 rats developed severe glomerulosclerosis, with fibrinoid necrosis and endarteritis proliferans consistent with transformation to a malignant hypertensive phenotype, an uncommon occurrence when maintained on a Hanover strain SD background as used in the present study. Although the development of malignant hypertension, in response to vandetanib, was confined to TGR(mRen-2)27 rats, two additional factors may have contributed to these findings. Firstly, SBP was higher in TGR(mRen-2)27 rats compared with SHRs. Secondly, vandetanib, as with most tyrosine kinase inhibitors, may also have "off-target" actions on other kinases that might have contributed to the observed effects. To address the issue of the different blood pressures between the rat strains, we considered the known effects of VEGF on vasorelaxation (22) and the hypertensive properties of anti-VEGF therapy (23) and accordingly administered a lower dose of vandetanib to TGR(mRen-2)27 rats. Despite similar SBPs between vehicle-treated TGR(mRen-2)27 rats and those that received the lower dose of vandetanib, renal injury was significantly worse in the latter group. To ascertain the potential contribution of off-target actions of vandetanib, we examined the effects of VEGF neutralization using an antibody-based approach that also resulted in the development of malignant hypertension. The extent of injury appeared greater with vandetanib than neutralizing antibody, even though the rise in blood pressure was lower with the former. This may reflect either pharmacodynamic and pharmacokinetic differences in the two treatment regimens or alternate modes of action.

A major finding of this study was that VEGF–VEGFR inhibition led to glomerular endothelial cell loss in normal animals that was incrementally increased by hypertension and an overactive RAS. This demonstrates that VEGF has a role not only in maintaining endothelial cell integrity in the physiological setting but especially in response to stress and that both hypertension and an overactive RAS are required for the development of malignant hypertension (24).

Significant structural changes were observed in podocytes after VEGF inhibition. In SHRs, these consisted principally of proteinaceous adsorption droplets, whereas TGR(mRen-2)27 rats displayed extensive changes of pseudocyst formation and adsorption droplet accumulation within the podocyte cell body with some foot process fusion. In contrast to the work of Sugimoto *et al.* (25), we found nephrin expression to be unchanged with VEGF inhibition,

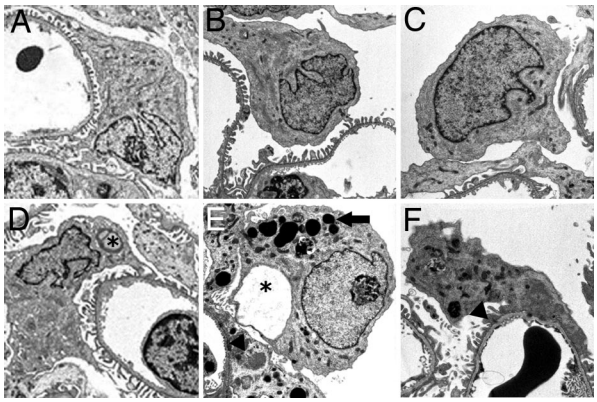

Fig. 6. Transmission electron micrographs of representative podocytes from vehicle-treated animals. (*A–C*) SD rat (*A*), SHR (*B*), and TGR(mRen-2)27 rat (*C*). (*D–F*) After vandetanib, SD rat (*D*), SHR (*E*), and TGR(mRen-2)27 rat (*F*). Among vandetanib-treated groups, SD rats had occasional podocyte pseudocysts (asterisk), SHRs showed a predominance of proteinaceous adsorption droplets (arrow) with occasional foot process fusion (arrowhead), and TGR(mRen-2)27 rats demonstrated severe podocyte injury with abundant adsorption droplet accumulation and some foot process fusion (arrowhead). (Magnification: ×6,600.)

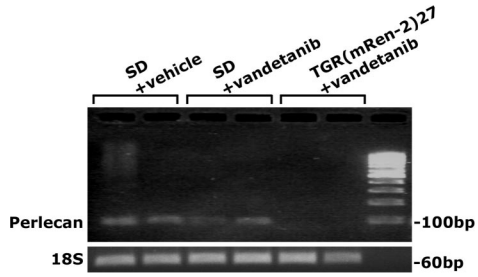

Fig. 7. RT-PCR for the heparan sulfate proteoglycan perlecan from microdissected glomeruli from SD rats + vehicle and SD and TGR(mRen-2)27 rats + vandetanib. Perlecan expression was undetectable in TGR(mRen-2)27 rats after vandetanib treatment.

when determined by quantitative *in situ* hybridization. We were unable to demonstrate Ret expression using real-time RT-PCR in glomeruli isolated by laser capture microdissection (LCM), consistent with previous reports in adult kidneys (26). However, it is plausible that either inhibition of Ret, expressed below the level of detection, or altered nephrin distribution may still contribute to the albuminuria observed.

Under physiological circumstances, the major barriers to the transglomerular passage of protein are the podocyte slit pore membrane and the glomerular basement membrane. Accordingly, in addition to exploration of the podocytes, we also examined one of the major contributors to the charge selectivity of the filtration barrier, perlecan (27). In contrast to untreated TGR(mRen-2)27 rats, perlecan mRNA was undetectable in glomeruli of TGR(mRen-2)27 rats that had received vandetanib. These findings raise the possibility that either endothelial cell loss or altered gene expression may contribute to the reduction in glomerular permselectivity observed in vandetanib-treated animals. Increased perlecan expression has been proposed as a mechanism for reduced albuminuria in diabetic PKC-$\alpha^{-/-}$ mice (28) although the role of heparan sulfate proteoglycans in maintaining the glomerular filtration barrier remains controversial.

The present study has several limitations. In the first instance, measurement of SBP was based on tail-cuff plethysmography, and we cannot exclude a pathological effect of acute or transient changes in blood pressure associated with VEGF inhibition. Second, TGR(mRen-2)27 rats were markedly hypertensive and, without pharmacological lowering of blood pressure, we have not defined whether RAS activation alone is sufficient for renal injury in the setting of VEGF inhibition. Although the present studies demonstrate the importance of VEGF in maintaining endothelial integrity in response to hypertension and RAS activation, the precise molecular mechanisms by which renal injury occurs remain unresolved.

VEGF inhibition by circulating sFLT1 leads to endotheliosis and proteinuria in preeclampsia (29). Consistent with this, hypertension and proteinuria are side effects commonly encountered in the clinic with anti-VEGF therapy (23). By way of contrast, the present study demonstrates the potentially detrimental effects of administering anti-VEGF therapy in the presence of preexisting hypertension and RAS-activation. The findings of a deleterious effect of VEGF inhibition in these studies, as well as in conditional knockout mice (9), are in contrast to those in diabetic renal disease, which overall report a favorable effect (30, 31). This suggests that the role of renal VEGF may be contextual and directly influenced by one or several various attributes of the diabetic or hypertensive milieu.

Methods

***In Vitro* Experiments.** Human renal glomerular endothelial cells (ScienCell Research Laboratories, San Diego, CA) were serum-starved and preincubated with either vandetanib (1 μM) or vehicle (DMSO) before stimulation with VEGF (50 ng/ml for 5 min). Cell lysates were then subjected to immunoprecipitation for VEGFR-2 (Santa Cruz Biotechnology, Santa Cruz, CA) before SDS/PAGE and immunoblotting for phosphotyrosine (4G10; Upstate Biotechnology, Lake Placid, NY), stripping, and blotting for VEGFR-2 (Santa Cruz Biotechnology) (*SI Methods*).

Animals. ***Study 1. Glomerular VEGF expression.*** Twelve-week-old male SD, SHR, and heterozygous TGR(mRen-2)27 rats were killed, and VEGF and VEGFR-2 expression were quantified as detailed below.

Study 2. VEGFR-2 kinase inhibition. Eight-week-old male SD, SHR, and TGR(mRen-2)27 rats were randomized to receive either vehicle (polysorbate 80) [1% Tween 80 (Sigma, St. Louis, MO)] or vandetanib (AstraZeneca, Cheshire, U.K.) for 24 days. Vandetanib is a potent inhibitor of the VEGFR-2 tyrosine kinase (IC_{50} 0.04 μM), with excellent selectivity versus other kinases including VEGFR-1, erbB2, MEK, CDK-2, Tie-2, IGFR-1R, PDK, PDGFRβ, and AKT (IC_{50} range: 1.1–100 μM) (32). Animals were treated with vandetanib suspended in polysorbate 80 at a dose of 25 mg/kg or vehicle administered by once daily oral gavage.

Study 3. $VEGF_{164}$ neutralizing antibody in TGR(mRen-2)27 rats. Specific $VEGF_{164}$ neutralizing antibody (R & D Systems, Minneapolis, MN) or control normal goat IgG (R & D Systems) were administered to TGR(mRen-2)27 rats (n = 3 per group) at a dose of 100 μg twice weekly (33) by i.p. injection for 3 weeks. The anti-VEGF antibody used (no. AF564) is directed against recombinant rat $VEGF_{164}$ and neutralizes 30 ng/ml rat VEGF with a neutralization $dose_{50}$ of 0.2–0.6 μg/ml.

All rats were housed in a stable environment and allowed free access to tap water and standard rat chow as outlined (34). SBP was recorded in preheated rats by tail-cuff plethysmography (35). An average SBP reading was taken from at least three consecutive recordings over a 10-minute period. GFR was measured by single-shot 99m-technetium diethylenetriamine pentaacetic acid (Tc^{99m}-DTPA) clearance (36). For estimation of urine albumin excretion, rats were individually housed in metabolic cages for 24 h with free access to tap water and standard diet. Urine albumin excretion was determined by double-antibody RIA as reported (37), and urine protein was measured with the benzethonium chloride method on an Olympus analyzer. All experimental procedures adhered to the guidelines of the National Health and Medical Research Council of Australia's Code for Care and Use of Animals for Scientific Purposes and were approved by St. Vincent's Hospital Animal Ethics Committee, Melbourne, Australia.

Tissue Preparation and Histochemistry. Rats were anesthetized with an i.p. injection of pentobarbital sodium, 60 mg/kg (Boeringer–Ingelheim, North Ryde, NSW, Australia). The right renal artery was clamped and the kidney removed, decapsulated, sliced transversely, and immersed in 10% neutral buffered formalin (NBF) for 24 h. Blood film examination was performed in at least three rats per group by using Wright–Giemsa staining. Other tissues (heart, mesentery, brain, aorta, liver, lung, duodenum, spleen, and testes) were removed from at least three rats per group and fixed as described. Tissues were routinely processed, embedded in paraffin, and sectioned before staining in H&E, PAS, Masson's trichrome, or Martius scarlet blue.

Immunohistochemistry. Macrophages were identified by using anti-rat CD68 monoclonal antibody ED1 (Serotec, Raleigh, NC). Glomerular endothelial cells were recognized by the monoclonal antibody JG-12 (Bender Medsystems, Vienna, Austria), which binds to endothelial cells of blood vessels but not to lymphatics in rat kidney (20). Podocytes were identified by using a polyclonal antibody (C-19) against WT1 (Santa Cruz Biotechnology). Immunohistochemistry was performed as described (34). Normal goat serum instead of primary antisera served as the negative control.

Endothelial Cell Density. Changes in endothelial density were quantified as reported (38) by using computer-assisted image analysis (13, 39). The proportional glomerular area showing positive JG-12 immunostaining was measured from three sections per rat (n = 10 per group), providing in excess of 300 glomeruli per treatment group, giving an index of glomerular endothelial cell density (38).

Podocyte Density. Podocyte density was determined by both light and electron microscopy. For electron microscopic estimation, the Weibel–Gomez method was used (n = 3 per group) (40). This method, when performed on single electron micrograph sections, produces comparable estimates to the disector/fractionator technique (41). For light microscopy, WT1-positive cells were counted in 30 glomeruli per animal (n = 6 per group) (42). All glomeruli were studied at the level of the juxtaglomerular apparatus (magnification $\times$400).

Glomerulosclerosis Index. Estimation of the degree of glomerulosclerosis was performed by using a semiquantitative technique as described (43) (*SI Methods*).

***In Situ* Hybridization and Quantitative Autoradiography.** Quantitative *in situ* hybridization was performed by using antisense riboprobes specific for $VEGF_{164}$ (gift of Steven Stacker, Ludwig Institute, Melbourne, Australia), VEGFR-2, and nephrin as described (38, 44, 45). Film densitometry of autoradiographic images was performed by computer-assisted image analysis (46) (*SI Methods*).

Electron Microscopy. For transmission electron microscopic analysis, kidneys from three rats per group were perfusion-fixed in gluteraldehyde, processed in cacodylate buffer, postfixed in osmium tetroxide, and block-stained in uranyl acetate before embedding in epon-araldite as described (47) (*SI Methods*). Ultrathin sections were taken through at least three randomly selected glomeruli from each animal, stained with uranyl acetate and lead citrate, and examined by using a Philips CM100 transmission electron microscope (Biomedical EM Unit, Newcastle University). Representative micrographs of the filtration barrier were taken from each animal. A semiquantitative technique was used to estimate the number of podocyte abnormalities (adsorption droplets or pseudocysts) per unit area of glomerulus. At the same time, a micrograph of the complete glomerular profile was taken at low magnification ($\times$700) for the estimation of glomerular area by point counting (48).

LCM. LCM was performed as described (49). Briefly, formaldehyde-fixed kidney sections ($n = 3$ per group) of 8-μm thickness were affixed to glass object slides. Deparaffinization was performed in 100% xylene before rehydration in graded ethanol. After rinsing in H_2O, sections were stained in HistoGene staining solution (Arcturus, Mountain View, CA), rewashed, dehydrated in graded ethanol, and reimmersed in xylene before air drying. One hundred glomeruli were microdissected from each section under direct visualization using an Arcturus Pixcell II System and captured on CapSure Macro LCM caps (Arcturus). Total RNA isolation, DNase treatment, and reverse transcription were performed by using a Paradise Whole Transcript RT Reagent System (Arcturus) according to the manufacturer's protocol.

Real-Time Quantitative RT-PCR. Real-time RT-PCR was performed on an ABI Prism 7900HT Sequence Detection System (Applied Biosystems, Foster City, CA) using SYBR green. Sequences were designed to span exon–exon boundaries by using Primer Express software v1.5 (Applied Biosystems). Primers were obtained from ACGT Corp. (Toronto, ON, Canada) with 18S forward primer TCGAGGCCCTGTAATTGGAA, reverse primer CCCTCCAATGGATCCTCGTT; perlecan forward primer GATTGTCAGTGTGGTGTTCATCAA, reverse primer GTCCGCGTTCCCTTCAGAA; and Ret kinase forward primer AGAGCCCGCCGTTATGC, reverse primer GATGGAGACACCGCTGAACTC. Experiments were performed in triplicate, and data analysis was performed by using Applied Biosystems Comparative C_T method. After amplification, PCR products were run on 2% agarose gels.

Statistics. All data are shown as mean $\pm$ SEM unless otherwise stated. Comparison between vehicle treated groups was with ANOVA, followed by Tukey's post hoc comparison. The effect of intervention was tested by two-way ANOVA with a Bonferroni posttest. Analysis of survival at the end of the study period was with a modified Fisher's exact test. All statistics were performed by using GraphPad Prism 3.00 for Windows (GraphPad Software, San Diego, CA). A change was considered statistically significant if $P < 0.05$.

We thank Ms. M. Pacheco, Ms. J. Court, Ms. S. Mason, Ms. D. Squires, Ms. L. DiRago, Mrs. S. Glowacka, Dr. B. Michell, Mrs. V. Thompson, and Mrs. T. Davey for excellent technical assistance and Dr. S. E. Quaggin and Dr. R. J. Johnson for helpful discussions. A.A. was supported by a Samuel Leonard Simpson Fellowship in Endocrinology from the Royal College of Physicians (U.K.), the Diabetes Research and Wellness Foundation, and the Northern Counties Kidney Research Fund U.K. D.J.K. is a recipient of a Career Development Award from the Juvenile Diabetes Research Foundation International (JDRF). Studies were supported by Canadian Institutes of Health Research Team Grant 161997 and by the JDRF.

1. Ferrara N, Carver-Moore K, Chen H, Dowd M, Lu L, O'Shea KS, Powell-Braxton L, Hillan KJ, Moore MW (1996) *Nature* 380:439–442.
2. Shalaby F, Rossant J, Yamaguchi TP, Gertsenstein M, Wu XF, Breitman ML, Schuh AC (1995) *Nature* 376:62–66.
3. Schrijvers BF, Flyvbjerg A, De Vriese AS (2004) *Kidney Int* 65:2003–2017.
4. Kamba T, Tam BY, Hashizume H, Haskell A, Sennino B, Mancuso MR, Norberg SM, O'Brien SM, Davis RB, Gowen LC, *et al.* (2006) *Am J Physiol* 290:H560–H576.
5. Maharaj AS, Saint-Geniez M, Maldonado AE, D'Amore PA (2006) *Am J Pathol* 168:639–648.
6. de Castro Junior G, Puglisi F, de Azambuja E, El Saghir NS, Awada A (2006) *Crit Rev Oncol Hematol* 59:40–50.
7. Wilson JF (2004) *Ann Intern Med* 141:165–168.
8. Kitamoto Y, Tokunaga H, Tomita K (1997) *J Clin Invest* 99:2351–2357.
9. Eremina V, Sood M, Haigh J, Nagy A, Lajoie G, Ferrara N, Gerber HP, Kikkawa Y, Miner JH, Quaggin SE (2003) *J Clin Invest* 111:707–716.
10. Senger DR, Galli SJ, Dvorak AM, Perruzzi CA, Harvey VS, Dvorak HF (1983) *Science* 219:983–985.
11. Barleon B, Sozzani S, Zhou D, Weich HA, Mantovani A, Marme D (1996) *Blood* 87:3336–3343.
12. Ku DD, Zaleski JK, Liu S, Brock TA (1993) *Am J Physiol* 265:H586–H592.
13. Kim YG, Suga SI, Kang DH, Jefferson JA, Mazzali M, Gordon KL, Matsui K, Breiteneder-Geleff S, Shankland SJ, Hughes J, *et al.* (2000) *Kidney Int* 58:2390–2399.
14. Hara A, Wada T, Furuichi K, Sakai N, Kawachi H, Shimizu F, Shibuya M, Matsushima K, Yokoyama H, Egashira K, Kaneko S (2006) *Kidney Int* 69:1986–1995.
15. Remuzzi G, Bertani T (1998) *N Engl J Med* 339:1448–1456.
16. Campbell DJ, Rong P, Kladis A, Rees B, Ganten D, Skinner SL (1995) *Hypertension* 25:1014–1020.
17. Campbell DJ, Duncan AM, Kladis A, Harrap SB (1995) *Hypertension* 25:928–934.
18. Gruden G, Thomas S, Burt D, Zhou W, Chusney G, Gnudi L, Viberti G (1999) *J Am Soc Nephrol* 10:730–737.
19. Kitayama H, Maeshima Y, Takazawa Y, Yamamoto Y, Wu Y, Ichinose K, Hirokoshi K, Sugiyama H, Yamasaki Y, Makino H (2006) *Am J Hypertens* 19:718–727.
20. Kang DH, Hughes J, Mazzali M, Schreiner GF, Johnson RJ (2001) *J Am Soc Nephrol* 12:1448–1457.
21. Kang DH, Nakagawa T, Feng L, Johnson RJ (2002) *Am J Pathol* 161:239–248.
22. Yang R, Ogasawara AK, Zioncheck TF, Ren Z, He GW, DeGuzman GG, Pelletier N, Shen BQ, Bunting S, Jin H (2002) *Hypertension* 39:815–820.
23. Yang JC, Haworth L, Sherry RM, Hwu P, Schwartzentruber DJ, Topalian SL, Steinberg SM, Chen HX, Rosenberg SA (2003) *N Engl J Med* 349:427–434.
24. Fleming S (2000) *J Pathol* 192:135–139.
25. Sugimoto H, Hamano Y, Charytan D, Cosgrove D, Kieran M, Sudhakar A, Kalluri R (2003) *J Biol Chem* 278:12605–12608.
26. Lee DC, Chan KW, Chan SY (2002) *Oncogene* 21:5582–5592.
27. Morita H, Yoshimura A, Inui K, Ideura T, Watanabe H, Wang L, Soininen R, Tryggvason K (2005) *J Am Soc Nephrol* 16:1703–1710.
28. Menne J, Park JK, Boehne M, Elger M, Lindschau C, Kirsch T, Meier M, Gueler F, Fiebeler A, Bahlmann FH, *et al.* (2004) *Diabetes* 53:2101–2109.
29. Maynard SE, Min JY, Merchan J, Lim KH, Li J, Mondal S, Libermann TA, Morgan JP, Sellke FW, Stillman IE, *et al.* (2003) *J Clin Invest* 111:649–658.
30. Flyvbjerg A, Dagnaes-Hansen F, De Vriese AS, Schrijvers BF, Tilton RG, Rasch R (2002) *Diabetes* 51:3090–3094.
31. Chen S, Kasama Y, Lee JS, Jim B, Marin M, Ziyadeh FN (2004) *Diabetes* 53:2939–2949.
32. Hennequin LF, Stokes ES, Thomas AP, Johnstone C, Ple PA, Ogilvie DJ, Dukes M, Wedge SR, Kendrew J, Curwen JO (2002) *J Med Chem* 45:1300–1312.
33. Hasegawa T, Kosaki A, Shimizu K, Matsubara H, Mori Y, Masaki H, Toyoda N, Inoue-Shibata M, Nishikawa M, Iwasaka T (2006) *Exp Neurol* 199:274–280.
34. Kelly DJ, Chanty A, Gow RM, Zhang Y, Gilbert RE (2005) *J Am Soc Nephrol* 16:1654–1660.
35. Bunag RD (1973) *J Appl Physiol* 34:279–282.
36. Gilbert RE, Wilkinson-Berka JL, Johnson DW, Cox A, Soulis T, Wu LL, Kelly DJ, Jerums G, Pollock CA, Cooper ME (1998) *Kidney Int* 54:1052–1062.
37. Jerums G, Allen TJ, Cooper ME (1989) *Diabet Med* 6:772–779.
38. Kelly DJ, Hepper C, Wu LL, Cox AJ, Gilbert RE (2003) *Nephrol Dial Transplant* 18:1286–1292.
39. Lehr HA, Mankoff DA, Corwin D, Santeusanio G, Gown AM (1997) *J Histochem Cytochem* 45:1559–1565.
40. Weibel ER, Gomez DM (1962) *J Appl Physiol* 17:343–348.
41. White KE, Bilous RW (2004) *Kidney Int* 66:663–667.
42. Kuhlmann A, Haas CS, Gross ML, Reulbach U, Holzinger M, Schwarz U, Ritz E, Amann K (2004) *Am J Physiol* 286:F526–F533.
43. Saito T, Sumithran E, Glasgow EF, Atkins RC (1987) *Kidney Int* 32:691–699.
44. Gilbert RE, Vranes D, Berka JL, Kelly DJ, Cox A, Wu LL, Stacker SA, Cooper ME (1998) *Lab Invest* 78:1017–1027.
45. Kelly DJ, Aaltonen P, Cox AJ, Rumble JR, Langham R, Panagiotopoulos S, Jerums G, Holthofer H, Gilbert RE (2002) *Nephrol Dial Transplant* 17:1327–1332.
46. Baskin DG, Stahl WL (1993) *J Histochem Cytochem* 41:1767–1776.
47. Jones SE, White KE, Flyvbjerg A, Marshall SM (2006) *Diabetologia* 49:191–199.
48. White KE, Bilous RW (2000) *J Am Soc Nephrol* 11:1667–1673.
49. Cohen CD, Grone HJ, Grone EF, Nelson PJ, Schlondorff D, Kretzler M (2002) *Kidney Int* 61:125–132.